

ORIGINAL RESEARCH

Open Access



Damping forced oscillations in power system via interline power flow controller with additional repetitive control

Shirui Feng^{1*} , Xi Wu², Zhenquan Wang¹, Tao Niu¹ and Qiong Chen²

Abstract

With the continuous expansion of power systems and the application of power electronic equipment, forced oscillation has become one of the key problems in terms of system safety and stability. In this paper, an interline power flow controller (IPFC) is used as a power suppression carrier and its mechanism is analyzed using the linearized state-space method to improve the system damping ratio. It is shown that although the IPFC can suppress forced oscillation with well-designed parameters, its capability of improving the system damping ratio is limited. Thus, combined with the repetitive control method, an additional repetitive controller (ARC) is proposed to further dampen the forced power oscillation. The ARC control scheme is characterized by outstanding tracking performance to a system steady reference value, and the main IPFC controller with the ARC can provide higher damping, and further reduce the amplitude of oscillations to zero compared with a supplementary damping controller (SDC). Simulation results show that the IPFC with an ARC can not only greatly reduce the oscillation amplitude, but also actively output the compensation power according to the reference value of the ARC tracking system.

Keywords: Forced oscillation, Interline power flow controller (IPFC), Additional repetitive control (ARC), Linearized state-space method

1 Introduction

With the continuous expansion of power systems and the application of power electronic equipment, system oscillation in the power grid gradually increases [1]. As one of the key problems affecting the safety and stability of power system, it is of great significance to carry out theoretical analysis of forced oscillation and develop specific suppression methods.

Forced oscillation is caused by periodic disturbances [2], with its amplitude inversely related to the system damping [3], while the oscillation rapidly decays as the disturbance source disappears [4]. In view of the above characteristics, several measures have been proposed for forced oscillation suppression. Although the source of

forced oscillation disturbances can be identified and removed through online system operating data [5, 6], the wavelet ridge technique [7] and spectral Granger causality analysis [8], the current forced oscillation identification technology is still in the development stage without guaranteed accuracy and timeliness. In addition, a power system stabilizer (PSS) [9] and some flexible AC transmission system (FACTS) equipment, such as a static synchronous series compensator (SSSC) [10], and static synchronous compensator (STATCOM) [11] are recommended for system damping. Under the Robust Exact Differentiator (RED) control strategy, a DFIG wind turbine equipped with energy storage can also further suppress inter-area oscillations [12]. As the source of forced disturbance continuously injects disturbance into the power system, the dampers proposed in [2, 13] can only reduce the oscillation amplitude without suppressing the forced oscillation completely.

* Correspondence: fengshirui@jspdi.com.cn

¹Jiangsu Electric Power Design Institute Co. Ltd, China Energy Engineering Group Co. Ltd, Nanjing, China

Full list of author information is available at the end of the article



© The Author(s). 2021 **Open Access** This article is licensed under a Creative Commons Attribution 4.0 International License, which permits use, sharing, adaptation, distribution and reproduction in any medium or format, as long as you give appropriate credit to the original author(s) and the source, provide a link to the Creative Commons licence, and indicate if changes were made. The images or other third party material in this article are included in the article's Creative Commons licence, unless indicated otherwise in a credit line to the material. If material is not included in the article's Creative Commons licence and your intended use is not permitted by statutory regulation or exceeds the permitted use, you will need to obtain permission directly from the copyright holder. To view a copy of this licence, visit <http://creativecommons.org/licenses/by/4.0/>.

In view of the periodic characteristic of the forced oscillation disturbance source, repetitive control technology is considered in this paper. This is based on the principle of an internal model. When the interference is found to be a periodic signal of known frequency, repetitive control can be used to track the system reference value accurately. Therefore, repetitive control is now widely used to deal with harmonic distortion caused by nonlinear load [14–16] or grid-tied inverters [17, 18]. However, repetitive control has not been widely applied to the analysis and research of suppressing power oscillation. Integrated with a carrier that can adjust the active and reactive power flow of the system, repetitive control can track the system steady-state reference value under the disturbance of forced oscillation.

As an advanced third generation FACTS device, an IPFC can play a more comprehensive and prominent role than a unified power flow controller (UPFC) in power flow regulation [19]. In this paper, an additional repetitive control (ARC) scheme of an IPFC is designed for suppressing forced oscillation in a power system. Based on the internal model principle of repetitive control, the IPFC is able to track the system power steady-state reference value and suppress the system forced power oscillation effectively.

2 Methods

In this article, an interline power flow controller (IPFC) equipped with an additional repetitive controller (ARC) is used as a power suppression carrier to suppress forced oscillation. Its mechanism and controller parameters are analyzed using the linearized state-space method. To verify the performance of ARC, an equivalent four-machine system including IPFC and forced oscillation source are constructed in MATLAB/SIMULINK. From the analysis and simulation, it has been found that the main IPFC controller with ARC can provide higher damping, and further reduce the amplitude of oscillations to zero compared with an IPFC based on a supplementary damping controller (SDC).

3 Principle of suppressing forced oscillation with IPFC

3.1 Principle of suppressing forced oscillation in a power system

A single-machine infinite system is used to analyze the situation of forced power oscillation. By solving the generator rotor motion equations, the change trend of power angle δ is represented as [3]:

$$\Delta\delta(t) = \frac{\Gamma \sin\omega_d t / K}{\sqrt{[(\omega_d/\omega_n)^2 - 1]^2 + (2\zeta\omega_d/\omega_n)^2}} \quad (1)$$

where $\Gamma \sin\omega_d t$ refers to the periodic disturbance source

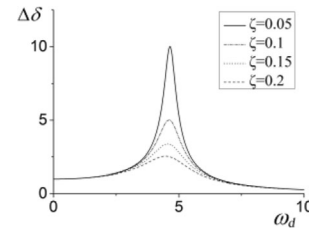


Fig. 1 Variation of power angle amplitude with disturbing source frequency under different damping ratios

with amplitude Γ and angular frequency ω_d . $\omega_n = \sqrt{K/T_J}$ refers to the generator natural frequency, K is the synchronous torque coefficient of the generator, and T_J is the inertia constant of the generator. $\zeta = D/2T_J\omega_n = D/2\sqrt{KT_J}$ is the damping coefficient and D is the generator damping.

According to (1) and assuming $\Gamma = 1$, $K = 1$, and $\omega_n = 4.65$ rad/s, the relationships between the power angle amplitude and ω_d of the disturbance source under different system damping ratios are shown in Fig. 1.

The following conclusions can be obtained from Fig. 1.

- 1) The closer ω_d and ω_n are, the more severe the forced oscillation will be.
- 2) By increasing the system damping ratio, the forced oscillation amplitude can be reduced.

Thus, if the system damping ratio approaches infinity, the change in power angle will approach zero and the forced oscillation can be completely suppressed. However, the system damping ratio cannot be increased infinitely in reality. For an independent power system, if the sum of the real parts of the eigenvalues of the state equation is invariant, the total damping of each mode of the system will remain constant [20]. If the damping of the electromechanical mode is increased to suppress the forced oscillation at a certain frequency, the damping of other electromechanical and non-electromechanical modes will be reduced accordingly. This may lead to low-frequency oscillations in other modes or large fluctuations of non-mechanical variables. Moreover, with the increase of the damping ratio, the reduced oscillation amplitude with the same damping ratio increment approaches zero. Therefore, it will be increasingly difficult to continue suppressing the forced oscillation using the same method. Thus, increasing the system damping can only reduce the forced oscillation amplitude to a certain extent, and other targeted suppression methods are required.

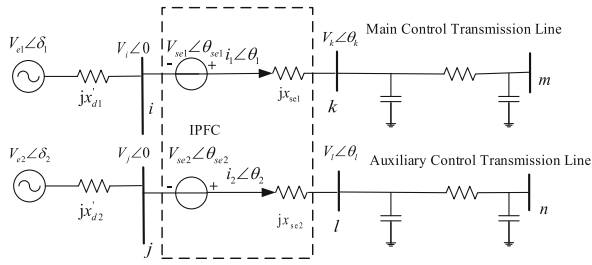


Fig. 2 Single-machine infinite-bus system with IPFC

3.2 IPFC dynamic performance analysis

In addition to quickly adjusting the line power flow and node voltage, the IPFC can also improve the transient stability of the power system by means of its dynamic adjustment function. In order to further analyze its dynamic adjustment mechanism, the IPFC power model is connected to two single-machine infinite-bus systems as shown in Fig. 2 with the detailed parameters listed in Appendix A. Simplified voltage sources are used to represent the IPFC series side converters.

As shown in Fig. 2, the upper line is the main control transmission line, whose active and reactive power are controlled by the IPFC. The lower line is the auxiliary control transmission line, which is used to maintain the stability of the DC capacitor voltage. Taking the main control line for example, the injected power of the IPFC will change the line active and reactive power flow, which can be represented as:

$$P_{ik} = \frac{V_{e1}V_i \sin\delta_1}{x'_{d1}} + \frac{V_\phi V_i}{x_{se1}} \quad (2)$$

$$Q_{ik} = \frac{V_{e1}^2 - V_{e1}V_i \cos\delta_1}{x'_{d1}} + \frac{V_\chi V_i}{x_{se1}} \quad (3)$$

where $V_\phi = V_{se1} \sin \theta_{se1}$ refers to the IPFC active power injection component and $V_\chi = V_{se1} \cos \theta_{se1}$ refers to the IPFC reactive power injection component.

The IPFC dynamic performance depends on the proportional-integral (PI) controller of the series converter. The relationship among the IPFC power injection components V_ϕ , V_χ and the line transmission power P_{ik} , Q_{ik} can be given as:

$$\begin{cases} V_\phi = (P_{ref} - P_{ik})(K_{\phi p} + K_{\phi i}/S) \\ V_\chi = (Q_{ref} - Q_{ik})(K_{\chi p} + K_{\chi i}/S) \end{cases} \quad (4)$$

where $K_{\phi p}$ and $K_{\phi i}$ refer to the respective proportional and integral gains of the PI controller used to control V_ϕ while $K_{\chi p}$ and $K_{\chi i}$ are the corresponding

proportional and integral gains of the PI controller used to control V_χ .

Equation (4) can be linearized as:

$$\begin{cases} \Delta V_\phi = -\Delta P_{ik}K_{\phi p} - \Delta P_{ik}K_{\phi i} \\ \Delta V_\chi = -\Delta Q_{ik}K_{\chi p} - \Delta Q_{ik}K_{\chi i} \end{cases} \quad (5)$$

Considering the inject active power from the IPFC, the motion equations of the generator rotor can be represented as:

$$\begin{cases} T_{J1} \frac{d\omega_1}{dt} + P_{e1} + P_{is} = P_{T1} - D_1(\omega_1 - 1) \\ \frac{d\delta_1}{dt} = \omega_1 - 1 \end{cases} \quad (6)$$

where $P_{is} = V_\phi V_i / x_{se1}$ indicates the IPFC active power injection into bus i .

Equation (6) can also be linearized as:

$$T_{J1} \frac{d^2\Delta\delta_1}{dt^2} + D_1 \frac{d\Delta\delta_1}{dt} + K\Delta\delta_1 + \frac{V_i}{x_{se1}}\Delta V_\phi = 0 \quad (7)$$

The system linearization model and transfer function block diagram can be obtained by considering (2)-(7), as shown in Fig. 3. The detailed parameters are listed in Appendix A.

The system linearization model, as shown in Fig. 3, is changed by the dynamic regulation of the IPFC. Therefore, with well-designed parameters, the IPFC is available to improve system damping and suppress forced oscillation. However, it has been proved that improving the system damping ratio has limited capability. Thus, in this paper, combined with the repetitive control method, an improved strategy is proposed to further suppress the forced power oscillation.

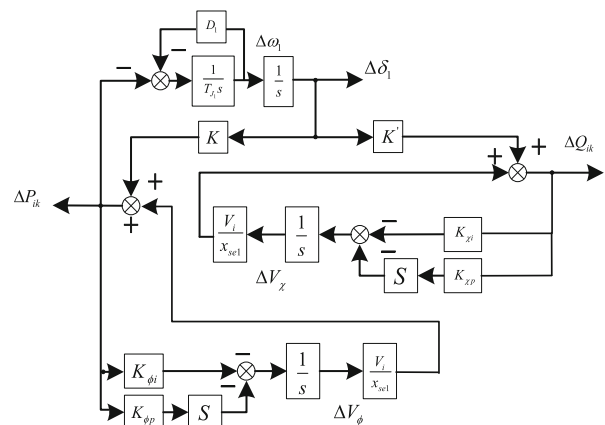


Fig. 3 Block diagram of system transfer function with IPFC

4 Forced oscillation suppressed by repetitive control

Repetitive control is a new control method based on the principle of an internal model. If a signal can be regarded as the output of an autonomous system, and the model of the signal is set in a stable closed-loop system, the feedback system will be able to track or suppress the signal completely [21]. The ideal transfer function of repetitive control can be deduced as follows, where e^{-sT} refers to the time prolonging link:

$$G_r(s) = \frac{e^{-sT}}{1 - e^{-sT}} \tag{8}$$

Assuming that the external interference is an input signal with period of T_d , the internal model of the input signal can be generated after a time prolonging link in the closed loop by setting the parameter $T = T_d$. Therefore, in theory, the internal model of repetitive control is able to track the system reference value without steady-state error.

The time-delay positive feedback loop of the repetitive control is able to correct the next control output using the control output of the previous cycle and the current error. Under ideal conditions, when the parameter of the time prolonging link T is equal to the period of the external forced disturbance signal T_d , the suppression effect will be optimal. However, because the pole is on the imaginary axis, the system is in a critical stable state, which may lead to poor stability and controllability.

A correction link $B(s)$ is introduced to overcome the above shortcoming. The pole of the repetitive controller is designed to drift slightly off the imaginary axis, and as a result, its stability is improved without sacrificing the restraining ability. Considering the fact that forced disturbance in the system belongs to low-frequency oscillation, the correction link should not shift the poles of the low frequency components. Thus, a first-order low-pass filter with a transfer function of $1/(ks + 1)$ is recommended as shown in Fig. 4.

The repetitive control and the original control structure are added in parallel to ensure their independence, and to reduce the impact on the original control system. The modified system structure is referred to as additional repetitive control (ARC), and its transfer function

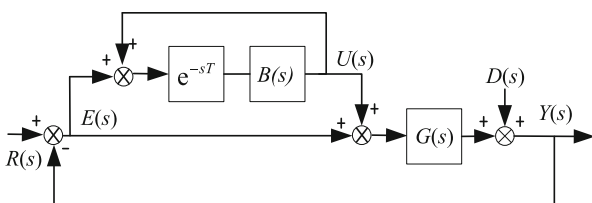


Fig. 4 Structure of ARC

block diagram is shown in Fig. 4. The line power steady-state input reference value is $R(s)$, while the line power actual value is $Y(s)$. The forced disturbance source with known oscillation period T_d is adopted as the external periodic disturbance source $D(s)$, $G(s)$ represents the transfer function of the original control system, and $E(s)$ represents the error of the controlled object.

The control equation of the ARC structure shown in Fig. 4 is given by:

$$\begin{cases} R(s) - Y(s) = E(s) \\ [E(s) + U(s)]G(s) + D(s) = Y(s) \\ U(s) = E(s) * C(s) \\ C(s) = e^{-sT}B(s)/1 - e^{-sT}B(s) \end{cases} \tag{9}$$

In order to simplify the analysis, $B(s)$ is taken as a constant of 1. Based on (9), $E(s)$ can be expressed as:

$$E(s) = \frac{R(s) - D(s)}{1 + [1 + C(s)] * G(s)} \tag{10}$$

The angular frequency of the forced power oscillation disturbance source $D(s)$ is set as $\omega_d = 2\pi/T_d$. Assuming $s = j\omega_d$ and $T = T_d$, there is:

$$\lim_{\omega \rightarrow \omega_d} C(j\omega_d) = \frac{1}{\frac{1}{e^{j\omega_d T_d}} - 1} = \infty \tag{11}$$

Substituting (11) into (10) yields:

$$\lim_{\omega \rightarrow \omega_d} E(j\omega_d) = 0 \tag{12}$$

From the above analysis, for the forced disturbance source with the frequency of $\omega_d/2\pi$, considering that T and $B(s)$ are equal to T_d and 1 respectively, the zero steady-state error tracking of the system can be theoretically achieved by ARC and the forced oscillation signal can be completely suppressed. The pole distribution of $C(s)$ is shown in black marks in Fig. 5. They are all located on the imaginary axis (assuming the frequency of the forced disturbance source is 1.35 Hz).

If $B(s)$ is not a constant of 1, and, for example, it is designed as $1/(ks + 1)$, $C(s)$ can be derived as:

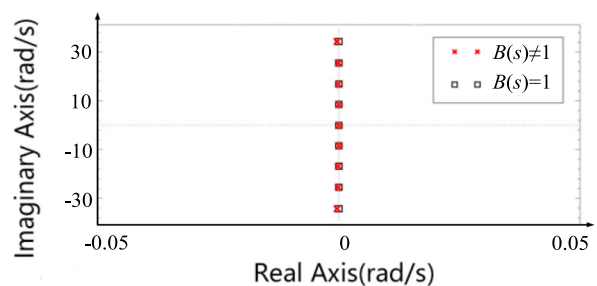


Fig. 5 Pole Distribution of $C(s)$

$$C(s) = \frac{e^{-sT} \frac{1}{ks+1}}{1 - e^{-sT} \frac{1}{ks+1}} \quad (13)$$

Expanding (13) with Euler’s equation and taking its modulus at $\omega = \omega_d$ yield:

$$\begin{aligned} |C(j\omega_d)| &= \frac{\sqrt{\cos^2 T_d \omega_d + \sin^2 T_d \omega_d}}{\sqrt{(1 - \cos T_d \omega_d)^2 + (k\omega_d + \sin T_d \omega_d)^2}} \\ &= \frac{1}{k\omega_d} \end{aligned} \quad (14)$$

When k is small and ω_d is in the low frequency band, the modulus of $C(s)$ is still near its maximum value. Therefore, when substituting $C(s)$ into the error expression, as shown in (10), the conclusion of (12) can still be established. In contrast, when ω_d is in the high frequency band, the error $E(s)$ will gradually increase with the decrease of the modulus of $C(s)$. For both cases, setting the constant k as $6E-3$, the $C(s)$ poles are shown with marks in Fig. 5. As seen, the poles in the low frequency band and the black marks almost overlap each other, while the poles in the high frequency band slightly deviate from the imaginary axis.

Overall, the poles of $B(s) = 1$ and $B(s) \neq 1$ are relatively close, which is consistent with the results obtained from the previous theoretical analysis. Based on the forced mechanism, the low-frequency oscillation generally occurs in the angular frequency range of $0.628 \sim 15.7$ rad/s, and ARC can output a more accurate internal model in the low frequency band. In this case, as long as k is made as small as possible and within the selectable range, $B(s)$ will have little impact on the suppression effect of forced oscillation, while enhancing the stability of the system. The variable k in $B(s)$ has to satisfy both (15) and (16) to ensure the stability of the system and the effective coverage of the low oscillation frequency band. The specific derivation process is discussed in Appendix B.

$$\left\| \left[1 + \frac{e^{-sT_d} \frac{1}{ks+1}}{1 - e^{-sT_d} \frac{1}{ks+1}} \right] G(s) \right\|_{\infty} < 1 \quad (15)$$

$$\begin{cases} |B(j\omega)| \approx 1, \omega \leq \omega_h \\ |B(j\omega)| < 1, \omega > \omega_h \end{cases} \quad (16)$$

5 Control scheme of IPFC for damping forced oscillations

5.1 Main controller design considering ARC

The ability of ARC in suppressing forced disturbance has been discussed. However, forced power oscillation continuously injects energy into the system, whereas

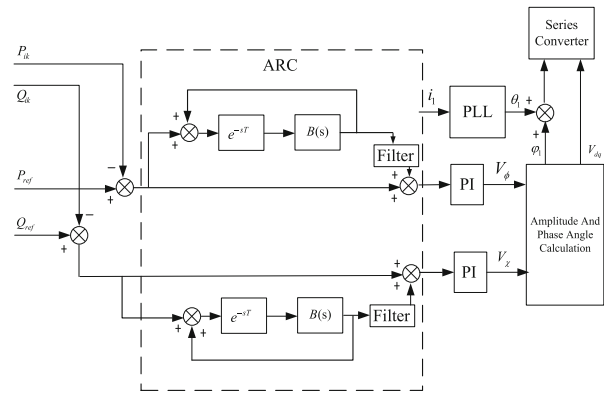


Fig. 6 Structure of IPFC main controller based on ARC

ARC itself does not have the ability for power adjustment. Therefore, combined with the IPFC as a power output carrier, ARC is used to track the system steady-state reference value.

The specific combination is shown in Fig. 6 where P_{ref} and Q_{ref} correspond to $R(s)$ while P_{ik} and Q_{ik} correspond to $Y(s)$. As the disturbance occurs inside the system, the response of the system to the forced oscillation is directly reflected in the line transmission power, while $D(s)$ is not marked in the controller structure. The ARC controller, shown in the dotted frame, consists of two channels, which are installed in the IPFC active and reactive control loops. As the ARC controller is added between the power comparison point and the original control system, it does not affect the forward channel of the PI control. This reduces interference to the original control system. A low-pass filter is added on the exit side of the additional controller to eliminate its effects, and to further prevent the effect of higher harmonics caused by repeated superposition of the repetitive controller.

The procedure of parameter selection is recommended to be as follows.

- 1) Obtain the line oscillation information through the wide area measurement system (WAMS);
- 2) The forced oscillation frequency ω_d is extracted from the line oscillation information with the TLS-ESPRIT (total least squares-estimation of signal parameters via rotational invariance technique) algorithm;
- 3) Calculate the period of the external forced disturbance signal T_d , thereby determining the initial prolonging link T in ARC;
- 4) To reduce the impact on the pole position of $C(s)$, k in $B(s)$ is chosen to be as small as possible while satisfying the requirements of

system stability and frequency coverage conditions outlined in Section 3;

- 5) Finally, fine tune T and k according to the actual simulation effect to achieve a good control effect.

5.2 The influence analysis of the auxiliary controller

As previously mentioned, the IPFC consists of two independent controllers, with the main controller designed to adjust the power through the main control transmission line in combination with ARC, and the auxiliary controller used to maintain a stable DC capacitor voltage. However, since the IPFC does not generate active power, the active power injected into the power line by the main converter and the auxiliary converter have to remain in dynamic balance, i.e.:

$$\begin{cases} P_{in1} = V_i V_{se1} \sin\theta_{se1} / x_{se1} \\ P_{in2} = V_j V_{se2} \sin\theta_{se2} / x_{se2} \\ P_{in1} + P_{in2} = 0 \end{cases} \quad (17)$$

where P_{in1} and P_{in2} refer to the injected active power of the main and auxiliary controllers, respectively.

From (17), it can be seen that the power injected from the main control line comes from the auxiliary control line. When forced oscillation occurs, the oscillating power of the main control line is transmitted to the auxiliary control line through the DC link. This is equivalent to increasing the damping of the original main control line. Therefore, the use of the IPFC can effectively suppress the forced oscillation of the main control line while the IPFC combined with ARC can further accomplish no-error tracking. However, the use of the IPFC impacts on the auxiliary

control line not originally affected by forced oscillation. Therefore, the damping characteristics of the system where the auxiliary control line is located are critical. If the system is overdamped, the oscillation power transferred by the IPFC will have little effect on the system. However, if the system is underdamped, the IPFC may expand the influence range of the forced oscillation.

In conclusion, the damping characteristics of the auxiliary control line should be carefully considered for the installation location of the IPFC.

6 Results and discussion

6.1 Case study

The validity of the proposed method is verified in an equivalent four-machine system based on MATLAB/SIMULINK, as shown in Fig. 7. Here, the main IPFC control converter is injected into the equivalent dual machine system, while the auxiliary converter is assumed to be connected to an infinite system. The parameters in Fig. 7 are described in Appendix C.

According to small disturbance analysis, the natural oscillation frequency of the system is 1.35 Hz. Without forced oscillation, the main controller can independently control the active and reactive power flow of the line, and the auxiliary controller can provide active power balance for the main line while maintaining the stability of the DC capacitor voltage.

The main IPFC control converter is installed between the buses of i and k with its power flow control target set to the original system steady-state power flow. The auxiliary IPFC control converter is installed between the

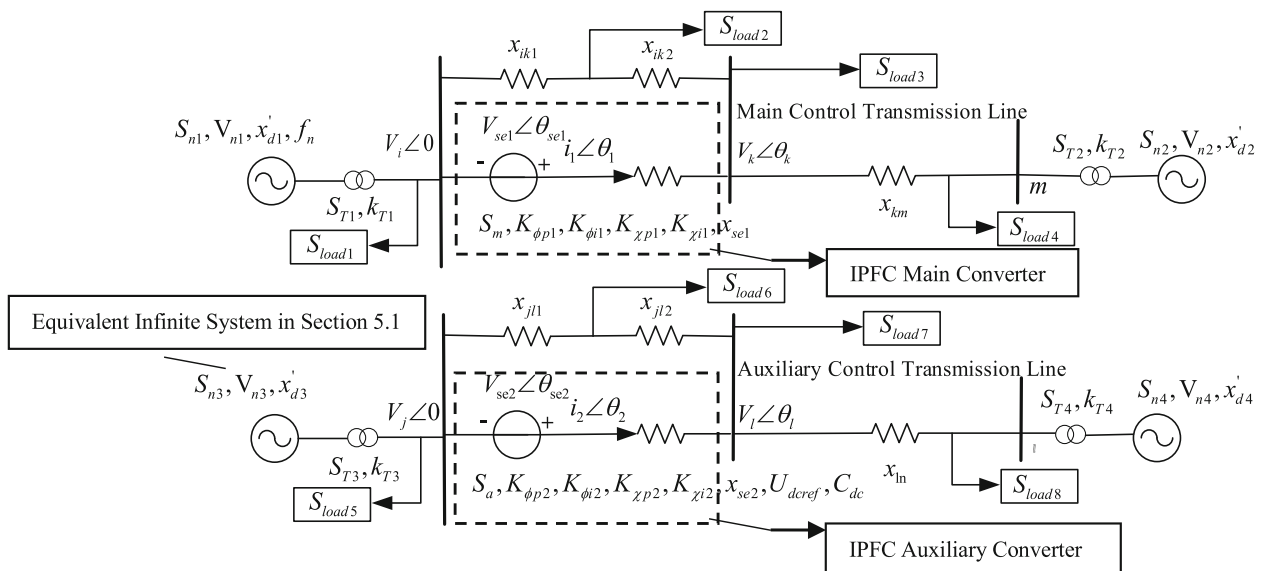


Fig. 7 An equivalent four-machine systems with IPFC

buses of j and l with its control target of maintaining a stable DC voltage.

A 1.35 Hz sinusoidal mechanical power disturbance with amplitude of 0.02 (standard unit value) is applied at the outlet of the G1 generator because forced oscillation caused by the generator power fluctuation is more serious than that from other disturbance sources. The expression of the disturbance is $d(t) = 0.02 \sin(2\pi * 1.35t)$. Simulations are carried out for four cases, i.e., without the IPFC, with the IPFC only, the IPFC based on a Supplementary Damping Controller (SDC) and the IPFC based on ARC. The SDC damping parameters are set according to the phase compensation method, and the designed parameters in Fig. 8 are described in Appendix C. The simulation results of P_{ik} are shown in Fig. 9, and the simulation results of P_{jl} and U_{dc} are illustrated in Fig. 10.

It can be seen from Fig. 9(a) that the dynamic adjustment of the IPFC enhances the system damping ratio and reduces the amplitude of forced oscillation. However, the effect is not sufficient to suppress the forced oscillation completely. The ARC parameters are determined using the design method described in Section 3 and the results of the IPFC with ARC are shown in Fig. 9(b). The period of external forced disturbance signal T_d is calculated as 0.7407 and the parameter k in $B(s)$ is set to 6E-3. The main IPFC controller with ARC provides higher damping and thus further reduces the amplitude of the oscillations. For periodic forced oscillation, the ARC controller can detect the difference of active power and further track the reference value. A feedback control signal is generated through the IPFC power tracking, and the oscillations in the system are largely suppressed to zero.

The main purpose of the SDC is to reduce the oscillation energy by adjusting the output phase-phase power waveform. From the comparison between ARC and SDC in Fig. 9(b), the compensation effect of the SDC slightly improves the oscillation suppression performance, while the IPFC based on ARC proposed in this paper accurately tracks the steady-state reference value of the system and generates the suppression power, resulting in a superior effect.

As can be seen from Fig. 10, the use of the IPFC negatively impacts on the auxiliary control circuit. The fluctuating power of the main controller is transferred to the auxiliary control side via the DC link. However, when the IPFC is not in operation, the oscillation power amplitude of the main control loop

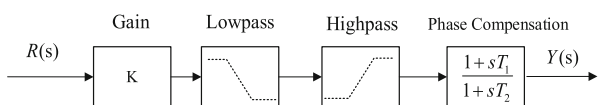


Fig. 8 Structure of SDC

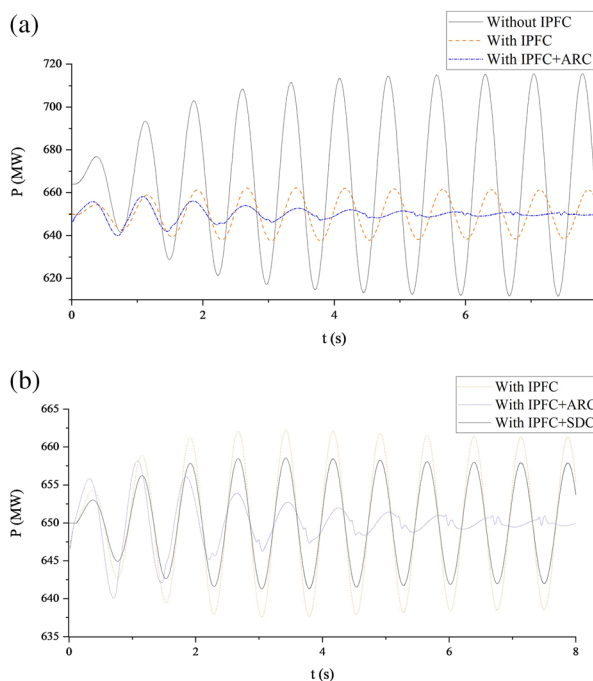


Fig. 9 Simulation results of P_{ik} of forced oscillation in the main control transmission line: **a** For cases: without IPFC, with IPFC only, and IPFC based on ARC; **b** For cases: with IPFC only, IPFC based on ARC, and IPFC based on ARC

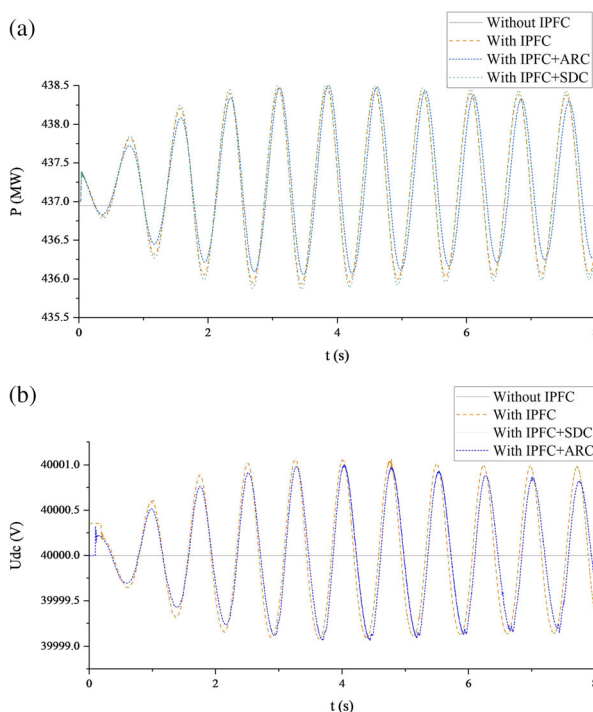


Fig. 10 Forced oscillation in the auxiliary control transmission line for three cases: without IPFC, with IPFC only, and IPFC based on ARC: **a** Simulation results of P_{ji} ; **b** Simulation results of U_{dc}

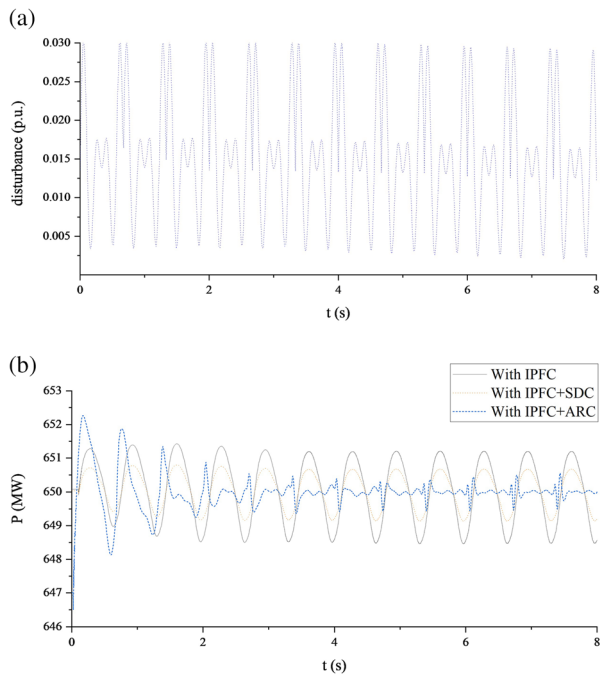


Fig. 11 Forced oscillation in the main control transmission line with complex disturbance: **a** Disturbance signal; **b** Simulation results of P_{ik} from two cases: with IPFC and IPFC based on ARC

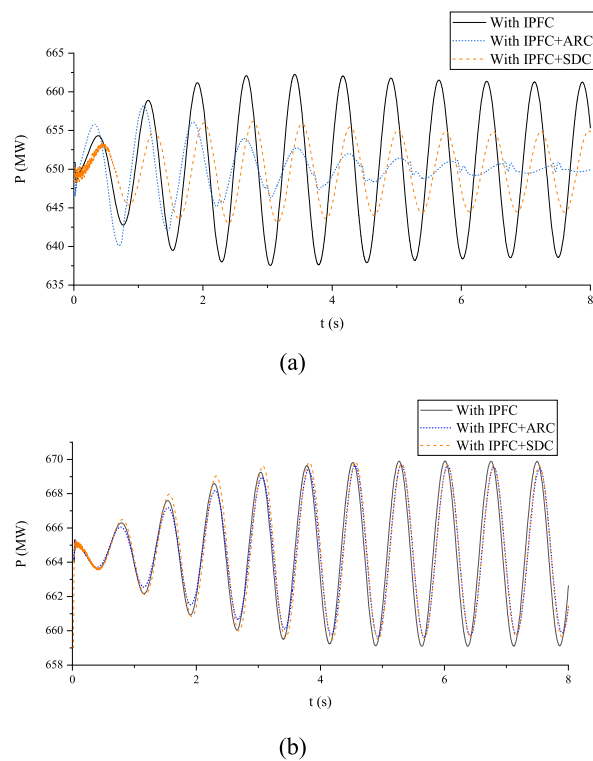


Fig. 12 Forced oscillation in transmission line: **a** Simulation results of P_{ik} ; **b** Simulation results of P_{jl}

will reach 50 MW, which can easily lead to system instability. With the IPFC in operation, the oscillation power amplitude of the main control line is attenuated to 12.5 MW, while the oscillation power amplitude of the auxiliary control line is only increased to 1.2 MW. Thus, the use of the IPFC has negligible influence on the auxiliary control line, while it effectively improves the safety and stability of the main control line.

Compared with the results under the IPFC with SDC, the IPFC with ARC reduces the main line oscillation power amplitude to 1.5 MW, while the power oscillation of the auxiliary control line remains unchanged. Thus, it can be concluded that the repetitive controller does not cause any deterioration to the auxiliary line, while it is able to effectively suppress the power fluctuation of the main control line.

In real systems, the disturbance signal of the power supply is more complicated, so a complex disturbance signal of 1.5 Hz shown in Fig. 11(a), is applied to the power supply terminal. From the simulation results in Fig. 11(b), it can be seen that the IPFC based on ARC can still accurately track and suppress the forced oscillation in the system.

In conclusion, the IPFC based on ARC can not only greatly reduce the amplitude of oscillation by increasing the system damping, but also actively output the

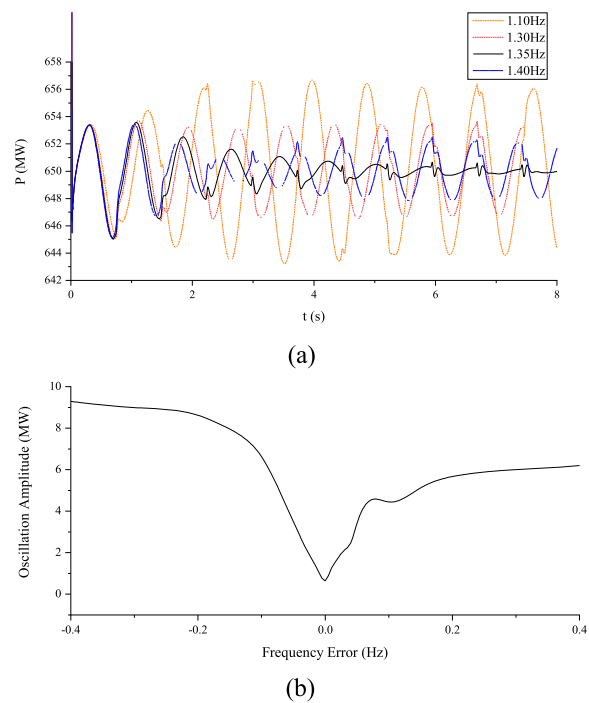


Fig. 13 Performance of ARC: **a** Simulation results of P_{ik} ; **b** Oscillation amplitude of P_{ik} under different frequency errors

compensation power according to the reference value of the ARC tracking system.

6.2 Discussion

As mentioned above, the greater the damping of the auxiliary line is, the lower the impact of forced oscillation will be. A more complicated case, as shown in Fig. 7, is proposed to verify the influence on the auxiliary line. The parameters of the dual-machine system connected with the auxiliary converter are consistent with the main control circuit. As in the case above, a sinusoidal mechanical power disturbance with the frequency of 1.35 Hz and amplitude of 0.02 (standard unit value) is applied at the outlet of the G1 generator. The simulation results of P_{ik} and P_{jl} are shown in Fig. 12.

The suppressed amplitude remains the same because of the unchanged parameters of the main control circuit when comparing the simulation results between Fig. 9(b) and Fig. 12(a). However, the auxiliary control line is changed from an over-damped infinite system to a weakly damped two-machine one, which is significantly affected by the forced oscillation. From the comparison between Fig. 10(a) and Fig. 12(b), the power amplitude of the auxiliary control line increases to 4.5 MW. Similarly, ARC also has a weak suppression effect to the auxiliary circuit. Therefore, it is recommended to choose an over-damped system for the installation of the auxiliary IPFC converter.

As mentioned above, the forced oscillation frequency is extracted from the line oscillation information with the TLS-ESPRIT. This is the critical factor for determining ARC parameters. To verify the robustness of the control system, deviations on the controller parameters are evaluated with the collected error of frequency information, and the simulation results are shown in Fig. 13.

From the internal model principle, ARC is proved to be sensitive to frequency change. As can be seen in Fig. 13(b), as the deviation of the acquisition frequency increases, the control performance of ARC declines, but is

still better than the case with only the IPFC. When the frequency deviation increases to 0.4 Hz, the control performances of ARC and SDC become similar. Therefore, precise acquisition of forced oscillation frequency is important to the control capability of ARC.

7 Conclusion

The mechanism of IPFC is analyzed based on the characteristics of forced oscillation to improve the system damping ratio and suppress forced oscillation. An ARC control scheme is designed for suppressing forced disturbances and tracking the steady-state reference value of the system effectively. Also, a method to generate IPFC suppressing power according to the ARC tracking requirement is introduced.

From the analysis and simulation, several findings are summarized as follows.

- 1) The main IPFC controller with ARC can provide higher damping, and further reduce the amplitude of oscillations to zero compared with an IPFC based on SDC.
- 2) The IPFC based on ARC can not only greatly reduce the amplitude by increasing the system damping ratio, but also actively output the compensation power according to the reference value of the ARC tracking system.
- 3) The ARC controller does not cause deterioration to the auxiliary line while suppressing the power fluctuation of the main control line effectively.
- 4) It is recommended to choose an over-damped system to install the auxiliary IPFC converter. This is able to better support the main control transmission line.

With the precise acquisition of forced oscillation frequency, ARC has a superior suppression effect for a single oscillation source. In practice, multiple forced oscillation sources have multiple oscillating frequencies so suppressing multiple frequencies is the future focus and research direction.

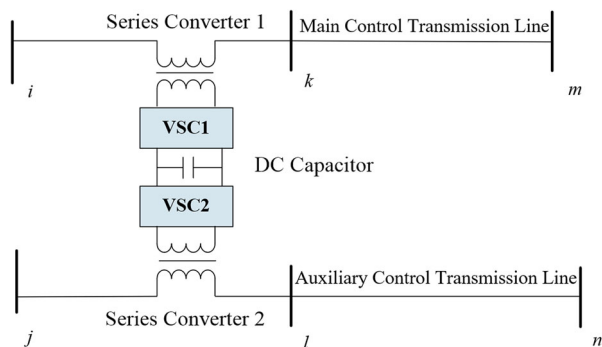


Fig. 14 Main structure of IPFC

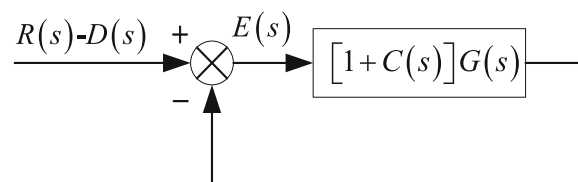


Fig. 15 Equivalent System of ARC

Table 1 Parameter descriptions and values

Name	Description	Value	Unit
S_{n1}/S_{n3}	The nominal power of Generator 1 and 3	2000	MVA
S_{n2}/S_{n4}	The nominal power of Generator 2 and 4	1400	MVA
$V_{n1} \sim V_{n4}$	The nominal voltage of Generator 1 ~ 4	13.8	kV
$x'_{d1} \sim x'_{d4}$	The transient reactance of Generator 1 ~ 4	0.296	
x_{d3}	The reactance of the infinite system	1.5E-4	H
f_n	The nominal frequency of the system	60	Hz
S_{T1}/S_{T3}	The nominal power of Transformer 1 and 3	2100	MVA
S_{T2}/S_{T4}	The nominal power of Transformer 2 and 4	1400	MVA
$k_{T1} \sim k_{T4}$	The transformer ratio of Transformer 1 ~ 4	13.8/500	
S_m/S_a	The nominal power of the main and auxiliary converter	100	MVA
x_{se1}/x_{se2}	The reactance of the main and auxiliary converter	0.26	H
$k_{\varphi p1}/k_{\chi p1}$	The proportional gain of main controller	3.75E-3	
$k_{\varphi i1}/k_{\chi i1}$	The integral gain of main controller	0.1875	
$k_{\varphi p2}$	The proportional gain of DC voltage controller of the auxiliary converter	3.75E-3	
$k_{\varphi i2}$	The integral gain of DC voltage controller of the auxiliary converter	0.1875	
$k_{\chi p2}$	The proportional gain of injected voltage controller of the auxiliary converter	1E-4	
$k_{\chi i2}$	The integral gain of injected voltage controller of the auxiliary converter	2E-2	
U_{dcref}	The nominal voltage of DC	40,000	V
C_{dc}	The total equivalent capacitance of DC link	3.75E-4	F
x_{ik1}/x_{ik2}	The reactance of the line between bus i and k	0.14	H
x_{jl1}/x_{jl2}	The reactance of the line between bus j and l	0.14	H
x_{km}	The reactance of the line between bus k and m	0.047	H
x_{ln}	The reactance of the line between bus l and n	0.047	H
S_{load1}/S_{load5}	The active power of load 1 and 5	250	MW
S_{load2}/S_{load6}	The active power of load 2 and 6	100	MW
S_{load3}/S_{load7}	The active power of load 3 and 7	2200	MW
S_{load4}/S_{load8}	The active power of load 4 and 8	50	MW
T_1	parameters of SDC	0.021	
T_2	parameters of SDC	0.665	

whose main structure is composed of multiple back-to-back voltage source converters (VSC) interconnected by DC capacitors, as shown in Fig. 14.

Two independent stand-alone infinity systems with IPFC, as shown in Fig. 2, consist of two series converters with different control goals. The detailed parameters are listed as follows.

- 1) V_{e1} , V_{e2} and δ_1 , δ_2 represent the voltage amplitudes and power angles of the two power sources, respectively; while x'_{d1} and x'_{d2} refer to the transient reactance of the sources.
- 2) The buses i , j , k , l , m and n represent different buses in the system. V_i , V_j , V_k , V_l refer to the voltage amplitudes, and θ_i , θ_j , θ_k , θ_l are the disparate voltage angles. Because the DC capacitor isolates the AC connection between the circuits, the two systems are independent of each other. Thus, θ_i and θ_j can be set to zero at the same time.
- 3) V_{se1} and V_{se2} are the injected voltage components of the main and auxiliary series converters, respectively; while θ_{se1} , θ_{se2} and x_{se1} , x_{se2} represent the voltage angles and reactance of the two series converters.
- 4) i_1 , i_2 and θ_1 , θ_2 represent the current amplitudes and the angles of the two transmission lines, respectively. P_{ik} and Q_{ik} refer to the active and reactive power of the main control line, and P_{ref} and Q_{ref} are the target power references of the series converter, respectively.

The specific variables of the system linearization model, as shown in Fig. 3, are introduced as follows.

- 1) P_{e1} and P_{T1} refer to the respective electromagnetic power and mechanical power of the generator in the main control transmission line, T_{J1} is the inertial time constant of the generator, D_1 is the damping coefficient and ω_1 is the angular velocity.
- 2) K and K' are the linearization constants of power angle δ_1 of active and reactive power, respectively, where $K = V_{e1} V_i \cos\delta_1 / x'_{d1}$, and $K' = V_{e1} V_i \sin\delta_1 / x'_{d1}$.

9 Appendix B

As described in Section 3, the specific derivation process of parameter k is shown as follows.

Based on (9), $E(s)$ can be further expressed as:

$$E(s) = -[1 + C(s)]G(s)E(s) + [R(s) - D(s)] \quad (\text{B1})$$

The structure corresponding to the transfer function in (B1) shown in Fig. 15, is the equivalent system of Fig. 4.

As the stability requirement of the equivalent system is $\| [1 + C(s)]G(s) \|_\infty < 1$, the parameter k should satisfy:

$$\left\| \left[1 + \frac{e^{-sT_d} \frac{1}{ks+1}}{1 - e^{-sT_d} \frac{1}{ks+1}} \right] G(s) \right\|_\infty < 1 \quad (\text{B2})$$

On the other hand, the pass band of $B(s)$ has to completely cover the frequency range of the low-frequency oscillations as:

$$\begin{cases} |B(j\omega)| \approx 1, \omega \leq \omega_h \\ |B(j\omega)| < 1, \omega > \omega_h \end{cases} \quad (\text{B3})$$

where ω_h refers to the highest frequency of the low-frequency oscillations of the forcing mechanism, and ω_h can be set as 4 Hz with a certain margin. Because the frequency range of the low-frequency oscillation of the forcing mechanism is very small, as long as k is small and within the range for maintaining the system stability, (B3) can be easily satisfied. Finally, considering the complexity of the actual system, k should also be fine-tuned according to the simulation results around the theoretical value to achieve a better suppression effect.

10 Appendix C

The descriptions and experimental values of the parameters in Figs. 7 and 8 are listed as follows.

Abbreviations

IPFC: Interline power flow controller; ARC: Additional repetitive controller; SDC: Supplementary damping controller; FACTS: Flexible AC transmission

system; PSS: Power system stabilizer; SSSC: Static synchronous series compensator; UPFC: Unified power flow controller; WAMS: Wide area measurement system; TLS-ESPRIT: Total least squares-estimation of signal parameters via rotational invariance technique

Acknowledgements

Not applicable.

Authors' contributions

Conceptualization, Shirui Feng and Zhenquan Wang; methodology, Tao Niu and Qiong Chen; software, Shirui Feng and Qiong Chen; writing—review and editing, Shirui Feng. All authors have read and agreed to the published version of the manuscript.

Authors' information

S. R. Feng (1992-), male, MD and Engineer, Major in renewable energy consumption, power system stability, smart grid and FACTS control technology.

X. Wu (1986-), male, PHD and Associate Professor, Major in power system stability and control, smart grid, renewable energy technology.

Z.Q. Wang (1980-), male, MD and Engineer, Major in renewable energy consumption, power system stability and smart grid, renewable energy technology.

T. Niu (1984-), male, MD and Engineer, Major in renewable energy consumption, power system stability and smart grid, renewable energy technology.

Q. Chen (1994-), female, MD, Major in FACTS control technology, power system stability and smart grid, renewable energy technology.

Funding

This research was funded by Jiangsu electric power company project "key technology research on planning and demonstration application of inter line power flow controller", J2020088.

Availability of data and materials

The datasets used and analysed during the current study are available from the corresponding author on reasonable request.

Declarations

Ethical approval

This article does not contain any studies with human or animal subjects performed by author.

Competing interests

The authors declare that they have no competing interests.

Author details

¹Jiangsu Electric Power Design Institute Co. Ltd, China Energy Engineering Group Co. Ltd, Nanjing, China. ²College of Electrical Engineering, Southeast University, Nanjing, China.

Received: 29 July 2020 Accepted: 19 May 2021

Published online: 22 June 2021

References

1. Ma, Y.-F., Zhou, Y.-C., Liu, H.-H., Liu, W.-D., Zhao, S.-Q., & Liu, J.-M. (2017). A local control method of multi-machine low frequency oscillation based on active disturbance rejection control. *Proceedings of the CSEE*, 37(5), 1360–1373.
2. Wilches-Bernal, F., Pierre, B.-J., Schoenwald, D.-A., Elliott, R.-T., Byrne, R.-H., Neely, J.-C., & Trudnowski, D.-J. (2020). Forced Oscillations in the Western Interconnection with the Pacific DC Intertie Wide Area Damping Controller. In *2020 IEEE Power & Energy Society Innovative Smart Grid Technologies Conference (ISGT)*, (pp. 1–5).
3. Tang, Y. (2006). Optical theory of forced power oscillation in power system. *Power System Technology*, 30(10), 29–33.
4. Ghorbaniparvar, M. (2017). A survey on forced oscillations in power system. *Journal of Modern Power Systems and Clean Energy*, 5(5), 671–682. <https://doi.org/10.1007/s40565-017-0273-4>.

5. Hua, Y., Liu, Y.-T., Zhang, P., & Du, Z.-C. (2017). Analysis and detection of forced oscillation in power system. *IEEE Transactions on Power Systems*, 32(2), 1149–1159.
6. Seppänen, J., Turunen, J., Nikkilä, A., & Haarla, L. (2018). Resonance of forcing oscillations and inter-area modes in the Nordic Power System. In *2018 IEEE PES Innovative Smart Grid Technologies Conference Europe (ISGT-Europe)*, (pp. 1–6).
7. Jha, R., & Senroy, N. (2019). Wavelet ridge technique based detection of forced oscillation in power system signal. *IEEE Transactions on Power Systems*, 34(4), 3306–3308. <https://doi.org/10.1109/TPWRS.2019.2909499>.
8. Luan, M., Li, S., & Gan, D. (2019). Locating forced oscillation source using granger causality analysis and delay estimation. In *2019 4th International Conference on Intelligent Green Building and Smart Grid (IGBSG)*, (pp. 502–507).
9. Wang, S.-K. (2013). A novel objective function and algorithm for optimal PSS parameter design in a multi-machine power system. *IEEE Transactions on Power Systems*, 28(1), 522–531. <https://doi.org/10.1109/TPWRS.2012.2198080>.
10. Zhao, Y., & Xiao, X.-N. (2007). Low-frequency oscillation of SSSC damping power system. *Automation of Electric Power Systems*, 31(17), 40–44.
11. Feng, S., Wu, X., Jiang, P., Xie, L., & Lei, J. (2018). Mitigation of power system forced oscillations: An E-STATCOM approach. *IEEE Access*, 6, 31599–31608. <https://doi.org/10.1109/ACCESS.2017.2784407>.
12. Tummala, A.-S.-L.-V. (2020). A robust composite wide area control of a DFIG wind energy system for damping inter-area oscillations. *Protection and Control of Modern Power Systems*, 3, 79–88.
13. Surinkaew, T., Shah, M. R., Muyeen, S. M., Nadarajah, M., Emami, K., & Ngamroo, I. Novel control design for simultaneous damping of inter-area and forced oscillation. *IEEE Transactions on Power Systems*, vol.36, pp. 451–463, 2021.
14. Sayem, A.-H.-M., Cao, Z.-W., & Man, Z.-H. (2017). Model free ESO-based repetitive control for rejecting periodic and aperiodic disturbances. *IEEE Transactions on Industrial Electronics*, 64(4), 3433–3441. <https://doi.org/10.1109/TIE.2016.2606086>.
15. Zou, Z., Zhou, K., Wang, Z., & Ming, C. (2015). Frequency-adaptive fractional order repetitive control of shunt active power filters. *IEEE Transactions on Industrial Electronics*, 62(3), 1659–1668. <https://doi.org/10.1109/TIE.2014.2363442>.
16. Long, J.-L., Zhen, J.-L., Ma, W.-C., Wei, D.-H., Wang, G.-Y., & Zhang, W.-H. (2020). Research on improved repetitive control strategy for shunt active power filter. *Proceedings of the CSU-EPSA*, 32(2), 132–139.
17. Zhao, Q.-S., Chen, S.-S., Zhou, X.-Y., Wang, X.-L., & Wang, S.-H. (2019). Analysis and design of combination controller based on repetitive control and proportional control for harmonics suppression of grid-tied inverters. *Transactions of China Electrotechnical Society*, 34(24), 5189–5198.
18. Wang, Z.-H., Zhao, D.-Z., Pang, D., Li, G.-Q., & Jin, G.-B. (2020). Optimization and performance analysis of predictive deadbeat repetitive control of three-level converter for power quality improvement. *Electric Power Automation Equipment*, 40(6), 121–127.
19. Wu, X., Wang, L., Chen, X., Liu, Y., Tao, J.-G., Teng, S., & Xuan, X. (2020). Comparative research on UPFC and IPFC enhancing transmission capability of a power system. *Power System Protection and Control*, 48(9), 128–134.
20. Zhao, S.-Q., Chang, X.-R., He, R.-M., & Ma, Y.-F. (2004). Borrow damping phenomena and negative damping effect of PSS control. *Proceedings of the CSEE*, 24(5), 7–11.
21. Zhang, K., Peng, L., Xiong, J., & Chen, J. (2006). State-feedback-with-integral control plus repetitive control for PWM inverters. *Proceedings of the CSEE*, 26(10), 56–62.

Submit your manuscript to a SpringerOpen[®] journal and benefit from:

- Convenient online submission
- Rigorous peer review
- Open access: articles freely available online
- High visibility within the field
- Retaining the copyright to your article

Submit your next manuscript at ► [springeropen.com](https://www.springeropen.com)
